# Antimicrobial Behavior of Biosynthesized Silica-Silver Nanocomposite for Water Disinfection: A Mechanistic Perspective

Thanusu Parandhaman[a,d,≠], Anisha Das[a,≠], B. Ramalingam[a], Debasis Samanta[b], T. P. Sastry[a], Asit Baran Mandal[c,d*] and Sujoy K. Das[a,d*]

[a]Bioproducts Laboratory, [b]Polymer Division, and [c]Chemical Laboratory, Council of Scientific and Industrial Research (CSIR)–Central leather Research Institute (CLRI), Chennai– 600020, India, and [d]Academy of Scientific and Innovative Research (AcSIR), New Delhi– 110001, India.
[≠]Both the authors have equal contribution

## Graphical Abstract

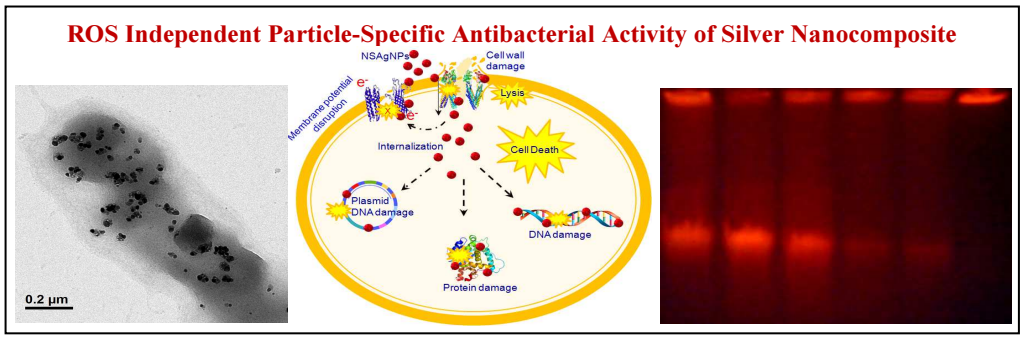


**Keywords**:

Silver nanomaterial,
Water disinfection,
Particle-specific activity,
Oxidative stress
Reactive oxygen species,
DNA damage

**Abstract:** The biosynthesis of nano-silica silver nanocomposite (NSAgNC) and it's as antibacterial effect on gram-negative bacteria viz. *Escherichia coli* and *Pseudomonas aeruginosa* has been investigated for disinfection of water. The as-synthesized NSAgNC exhibited antibacterial activity in a dose dependent manner and ~99.9% of *E. coli* and *P. aeruginosa* were killed at a concentration of 1.5 mg/mL of NSAgNC (5.1 wt% Ag) within 5 h. The NSAgNC showed similar antibacterial activities both in oxic and anoxic conditions. The results further demonstrated that NSAgNC exhibited reactive oxygen species (ROS) independent "particle specific" antibacterial activity through multiple steps in absence of leached out $Ag^+$ ions. The initial binding of NSAgNC on the cell wall caused loss of cell membrane integrity and leakage of cytoplasmic materials. Inhibition of respiratory chain dehydrogenase by NSAgNC caused metabolic inactivation of the cells and affecting the cell viability. Genomic and proteomic studies further demonstrated the fragmentations of both plasmid and genomic DNA and down regulation of protein expression in NSAgNC treated cells, which leading to the cell death. Thus the biosynthesized NSAgNC has great potential as disinfectant for water purification while minimizing the toxic effects.

[*]**Address for communication:** Dr. Sujoy K. Das and Prof. Asit Baran Mandal
Email: sujoy@clri.res.in; sujoydasiacs@gmail.com; abmandal@hotmail.com
Tel: +914424437133, +914424910846, Fax: +914424911589, +914424912150

## 1. Introduction

Access to a clean, safe and sustainable source of pure water is the crying need of the present century. Contamination of water with pathogenic microorganisms has detrimental effect on human health and aquatic species. According to U.S. EPA and WHO guidelines, potable water must be free from coliform microorganisms or a few may be present [1,2]. The common practices employing for treatment of water are neither safe nor cost effective. Most of the methods consume a significant amount of chemical agents, which often cause formation of harmful by-products raising health and environmental issues [3,4]. Moreover, it takes prolong time to get rid of bacterial pathogens.

Over the past few years increasing research efforts have been devoted to explore the nanotechnology to overcome the problems of water purification [5-7]. Due to broad spectrum antimicrobial activity, silver nanoparticles (AgNPs) have great application potential in disinfection of contaminated water [8,9], however, aggregation of AgNPs and leaching of $Ag^+$ ions in aquatic system restricted the application of AgNPs [10]. Therefore, demand for production of solid supported silver nanomaterials has been increased; however, synthesis and fabrication of supported of silver nanomaterial requires extensive use of toxic chemicals and organic solvents, which frequently raise health and safety issues [11,12]. The green synthesis of silver nanomaterial has recently gained significant importance as an alternative to reduce the toxic effects of hazardous materials. In spite of initial success in production of AgNPs using various types of uni- and multi-cellular organisms [13-16], biosynthesis of AgNPs on solid support has not been well documented. To enhance the application of biosynthesized AgNPs as it is or in the form of nanocomposite, it is prerequisite to understand the antibacterial mechanism of silver nanomaterials. The molecular mechanism of antibacterial activity of AgNPs however, has not well been understood; there is still debate on the mechanism of action. Several studies suggested that dissolution of $Ag^+$ ions from AgNPs is the main mechanism of the antibacterial activity of AgNPs [17-19]. The $Ag^+$ ions primarily bind with the cell membrane proteins, mostly respiratory enzymes, and denature the enzymes and interrupt the electron transport pathway causing cell death. Other studies have suggested that AgNPs kill the microorganism through a contact inhibition mode [20,21]. The permeability of the cell membrane increases by incorporation of AgNPs into the cell membrane and subsequently forms permeable pits leading to an osmotic collapse and releases the intracellular materials. Recently, few reports also proposed that oxidative stress induced reactive oxygen species (ROS) generation is the main mechanism of antibacterial activity of AgNPs [22,23]. The excessive production of ROS subsequently triggers sever damages in the cells including DNA and protein, leading to the cell death. Some other studies however, attributed that AgNPs exhibited “particle specific” activity, which is influenced by size, shape, surface charge, and solution chemistry of AgNPs [21]. The extent to which these factors influence the antimicrobial activity of AgNPs however, remains an open question.

To address the issues of green synthesis of solid supported AgNPs and antibacterial mechanism of silver nanomaterials, we demonstrated the biosynthesis of NSAgNC and explored the antimicrobial mechanism of the synthesized NSAgNC against gram-negative bacteria *i.e*. *Escherichia coli* and *Pseudomonas aeruginosa*. The effects of NSAgNC on the cell viability, ROS production and DNA fragmentation as well as protein expression were investigated to reveal the mechanism of action. Furthermore, the role of leached out $Ag^+$ ions in antibacterial activity of NSAgNC was eliminated by conducting the experiment under strictly anaerobic condition. The results further demonstrated for the first time that silver nanocomposite exhibited "particle specific" antibacterial activity in absence intracellular ROS production and dissociation of $Ag^+$ ions. Moreover, the biosynthesized NSAgNC prevents leaching of toxic $Ag^+$ ions and reduces the toxic effect of silver nanomaterials in the environment and aquatic species.

## 2. Experimental Section

### *2.1. Materials*

All chemicals and microbiological media were purchased from Sigma, and HiMedia, India, respectively. Nano-silica powder was a gift from SÜD-CHEMIE, Germany and used as received. The microorganisms were obtained from the Institute of Microbial Technology, Chandigarh, India.

### *2.2. Synthesis of NSAgNC*

Protein mediated synthesis of NSAgNC was carried out following the procedure as described earlier with some modification [24]. In brief, nano-silica powder (5 g) was added into $AgNO_3$ solution (200 mL, 5 mM) and incubated in shaking condition (120 rpm) for 5 h at 30 ± 1 °C. 25 mL protein extract (6 mg/mL) of *R. oryzae* was then added to the solution and incubated at 30 °C for another 48 h under similar condition. After completion of incubation, the material was separated by centrifugation (10,000 rpm for 15 min), washed with deionized and double distilled water several times to remove unreacted $Ag^+$ ions and finally dried at 50 °C in a hot air oven. The as-prepared NAgNC was characterized using UV-vis spectroscopy and transmission electron microscopy. The leaching of $Ag^+$ ions from NSAgNC was measured by fame atomic absorption spectrometer (AAS, Analytic Jena) against standard silver solution.

### *2.3. Characterization of NSAgNC*

The as-synthesized NSAgNC was dispersed in Millipore water (18.2 MΩ) by sonication for 20 min and UV-vis spectra was recorded on JASCO UV-vis spectrophotometer (V650 model) in the range of 250–800 nm. The dispersed solution of nano-silica was also recorded as control. The size and shape of the nanoparticles was studied through high resolution transmission electron microscopy (HRTEM)

analysis of the dispersed solution of NSAgNC. The dispersion was drop-casted on a copper grid (400 mesh size) and the microscopic images were recorded on a HRTEM instrument (JEOL JEM 2010) operated at an accelerating voltage of 200 kV equipped with an energy dispersive X-ray analysis (EDXA) system. The histogram of the particle size distribution (PSD) was measured from 140 nanoparticles recorded from multiples HRTEM images to calculate the average size of the AgNPs in NSAgNC. The surface charge of NSAgNC was measured through Zeta potential analysis of the dispersed solution of NSAgNC on Zetasizer (Malvern Zetasizer) at different pH values (2.0–10.0). The pH value of the dispersed solution was adjusted by addition of 1M HCl or NaOH solution, as required.

*2.4. Antimicrobial activity of NSAgNC*

Different amounts (0–2.0 mg/mL) of NSAgNC were added to sterile nutrient (5% beef extract, and 3% pepton) broth and inoculated separately with freshly grown *E. coli* and *P. aeruginosa*. The growth kinetics of *E. coli* and *P. aeruginosa* were then recorded for 30 h by collecting the samples at different time intervals and measured the optical density of the broth at 600 nm (denoting as $OD_{600}$) using a UV-vis spectrophotometer. Growth of bacteria in presence of nano-silica was performed as control experiment. The microbicidal activities of NSAgNC on these organisms were determined by standard plate count method. The experimental detail is provided in supporting data. The efficacy (killing %) of antibacterial activity of NSAgNC was determined using following equation:

Antibacterial efficacy (%) = $[(N_{\text{untreated}} - N_{\text{treated}})/ N_{\text{untreated}}] \times 100$, where $N_{\text{nntreated}}$ and $N_{\text{treated}}$ are numbers of viable cells grown on agar plate before and after treatment with NSAgNC, respectively. The same experiments were repeated under anaerobic condition keeping other parameters same to determine the effect of $Ag^+$ ions leached out from NSAgNC. At different time intervals cells were collected using a sterile syringe and number of viable cells was counted by plate count method as described above. The experimental detail is provided in supporting data. The cell viability of the treated cells was measured by MTT and LIVE/DAED kit assay (see Supporting data for details). The killing efficiency was determined as

Killing efficiency (%) = $[(OD_{590\text{negative control}} - OD_{590\text{treated}})/ (OD_{590\text{negative control}} - OD_{590\text{positive control}})] \times 100$, where negative and positive controls correspond to cells without any treatment and 70% isopropyl alcohol treated cells, respectively.

The alteration of the cellular morphology after treatment with NSAgNC was observed using HRTEM images. Bacterial cells were thoroughly washed with phosphate buffer (50 mM, pH 7.2), and fixed with 2.5% glutaraldehyde solution in the same buffer upon incubation for 5 h. The cells were then washed thrice with the same buffer followed by dehydration with graded (40-100%) ethanol series. The dehydrated cells were drop casted on carbon coated copper grids (400 mesh size) and micrographs were recorded on HRTEM instrument operated at an accelerating voltage of 100 kV.

*2.5. Intracellular reactive oxygen species (ROS) and glutathione (GSH) measurement*

Intracellular ROS production in the treated cells was measured by incubation of the cells with 2,7-dichlorofluoroscein diacetate ($H_2$-DCFDA), followed by fluorescence intensity measurement using a Varian Eclips spectrofluorometer with excitation and emission at 488 and 525 nm, respectively. The GSH concentration was determined by incubation of cells with 5,5′-dithio-bis-(2-nitrobenzoic acid) (DTNB) followed by absorbance measurement at 412 nm using U-vis spectrophotometer. Untreated and $H_2O_2$ (1 mM and 10 mM) treated cells were served as negative and positive control, respectively.

*2.6. Effect of surface charge of NSAgNC on antibacterial activity*

Dispersed suspension of NSAgNC was taken in different conical flasks and pH value of suspension was adjusted to 2.0–10.0 by addition of 1 M HCl or NaOH solution as required, followed by incubation for 20 min under shaking (120 rpm) to condition the NSAgNC. After completion of incubation, NSAgNC was collected, washed with sterile double distilled water and antibacterial activity was measured by plate count method as described above. The zeta potential of bacterial cell was also recorded on Zetasizer as described above.

*2.7. Metabolic activity and enzymatic activity of respiratory chain dehydrogenase*

The metabolic activity of the cells was determined by resazurin (Alamar Blue) assay. Both treated and untreated cells were incubated separately with 100 µL of 125 µg/mL resazurin solution for 1 h at 37 ± 1 °C. The conversion rate of resazurin to resorufin by living cells was assayed spectrophotometrically at 400–700 nm. The effect of NSAgNC on respiratory change enzyme lactate dehydrogenase activity was carried out by incubation of the treated cells with 100 µL of 50 mg/mL iodonitrotetrazolium chloride (INT) solution for 60 min at 37 ± 1 °C in dark. At the end of incubation, cells were collected and dissolved in 1 mL of acetone-ethanol (1:1 ratio) mixture. The dehydrogenase activity was then assayed through formazan formation by measuring absorbance of the extracted solution at 490 nm on UV-vis spectrophotometer. Untreated and $H_2O_2$ (10 mM) treated cells were served as positive and negative control, respectively.

*2.8. DNA fragmentation analysis and protein profile analysis*

The genomic and plasmid DNA was extracted from cells using standard protocol [25]. Following treatment with NSAgNC (0–2.0 mg/mL), cells were collected, washed with phosphate buffer (50 mM, pH 7.2) and then treated with lysis buffer (50 mM Tris-HCl pH 8.0, 10 mM EDTA, 20% sucrose, 0.5% Triton X-100 and 100 µg/mL lysozyme). Cell lysates were incubated with proteinase K (200 µg/mL) for 1 h at 37 °C. Both genomic and plasmid DNA were then extracted adopting standard protocols (see

supporting data for details) and analysed by 1.5% agarose gel electrophoresis followed by staining with ethidium bromide.

Similarly, intra and extracellular proteins were collected both from treated and untreated cells (see supporting data) and protein profiles were analyzed by standard 12% sodium dodecyl sulphate–polyacrylamide gel electrophoresis (SDS–PAGE).

All the experiments were performed minimum three times and details of the experimental procedures are provided in the supplementary data.

## 3. Results and Discussion

### *3.1. Synthesis of NSAgNC*

Environmentally sustainable one pot green synthesis of NSAgNC was carried out by protein mediated reduction of silver ion bound to the nano-silica surface without using any chemicals. The appearance of brown color following 48 h of incubation indicated the formation of NSAgNC, which showed absorption maximum at 418 nm (**Fig. 1A**) due to the Surface Plasmon Resonance (SPR) of AgNPs. The HRTEM image (**Fig. 1B**) of NSAgNC clearly depicted the synthesis of AgNPs on nano-silica surface. The PSD histogram pattern (Supporting data **Fig. S1**) of AgNPs was measured from 140 nanoparticles, which demonstrated average size of AgNPs is 20 ± 4.5 nm. The number nanoparticles were counted from several HRTEM images recorded from randomly selected different microscopic field across the representative sample. The zeta potential of NSAgNC at different pH values showed that NSAgNC carried a net positive surface charge at pH values <7.0 (**Fig. 1C**), while the energy dispersive X-ray analysis demonstrated that the as-synthesized NSAgNC contain 5.1 wt% Ag. The NSAgNC remained stable over a period of three months and did not show any aggregation of AgNPs as observed by the SPR band. The leaching of $Ag^+$ ions from NSAgNC was also analysed by AAS, however, the concentration of $Ag^+$ ions in aqueous solution was beyond the detection limit. The biosynthesized NSAgNC therefore, prevents leaching of $Ag^+$ ions giving stability to the synthesized AgNPs and protects the natural ecosystem from toxic effect of silver nanomaterials [10,26,27].

### *3.2. Antibacterial activity of NSAgNC*

The antibacterial activity of NSAgNC was tested against *E. coli* and *P. aeruginosa* in nutrient broth through turbidity measurement. Nutrient broth supplemented with different concentrations of NSAgNC (0–2.0 mg/mL) were inoculated with freshly grown bacterial culture and incubated at 37 °C for various time intervals (0–30 h) to investigate the effect of NSANC on growth of the organisms. The results (**Fig. 2A**, **C** and, Supporting data **Table S1**) showed that NSAgNC exhibited concentration dependent antibacterial activity and prevented bacterial growth at concentration of >1.0 mg/mL of NSAgNC. The

controlled experiments with nano-silica exhibited high turbidity due to bacterial growth. The NSAgNC (>1.5 mg/mL) containing media remained opaque still 72 h, indicating long term antibacterial activity of NSAgNC at a concentration of 1.5 mg/mL or more. The antibacterial activity of NSAgNC was further quantitatively evaluated by studying the bacterial growth kinetics (**Fig. 2B, D**), which was monitored by measuring the optical density at 600 nm ($OD_{600}$). The bacterial growth kinetics showed a typical dose-dependent antibacterial effect of NSAgNC. Compared to the growth curve of the bacteria in presence of nano-silica, NSAgNC significantly retarded the growth of both *E. coli* and *P. aeruginosa* at a concentration of NSAgNC above 1 mg/mL. The bacterial growth were completely inhibited when the concentration of NSAgNC increased to 2 mg/mL and 1.5 mg/mL, respectively in case of *E. coli* (**Fig. 2B**) and *P. aeruginosa* (**Fig. 2D**). Remarkably, the growth of both bacteria was completely inhibited during 72 h of incubation (**Fig. 2A, C**). It is therefore, reasonable to conclude that high stability of NSAgNC was responsible for the observed long-term antibacterial activity.

The bactericidal activity of NSAgNC was studied by plate count (**Fig. 3A**) and MTT assays (**Fig. 3B**) following incubation of bacterial cell with NSAgNC, which further demonstrated that NSAgNC exhibited both concentration and time dependent antibacterial activity. The cell viability assay of the treated cells demonstrated that killing efficiency increased with increase in concentration of NSAgNC as well as contact time. Results showed that ~70% of bacterial cells were killed at a concentration of 1 mg/mL of NSAgNC within 5 h of incubation and killing efficiency increased to ~80% when incubated for 8 h. However, the cell death increased to 90% within a contact time of 3 h when the concentration of NSAgNC was increased to 2 mg/mL (**Fig. 3C**) and as much as 99.9% of bacterial cells were killed at 5 h with same concentration. The concentration and time dependent antibacterial activity thus, suggested that interaction of NSAgNC with bacteria is necessary for NSAgNC mediated killing of bacterial cells. Results also demonstrated that NSAgNC showed excellent antimicrobial activity against the gram negative bacteria and killed as much as 99.9% of bacterial cells.

### *3.3. Oxidative stress and intracellular glutathion concentration*

The oxidative stress has been reported to play a major role in nanoparticles mediated cytotoxicity and genotoxicity in prokaryotic cells [28,29]. The interaction of metal nanoparticles with bacterial cells induces oxidative stress through production of ROS, such as hydroxyl radicals $OH^{\bullet}$, superoxide ions $O_2^{-\bullet}$, $H_2O_2$ and hydroperoxyl radicals, over the cellular antioxidant defences and damages to the protein and nucleic acids [22,23]. Therefore, the oxidative stress in the cells following treatment with NSAgNC was assayed through measurement of intracellular ROS production and GSH concentration. The intracellular production of ROS in the treated cells was determined by fluorometric assay using intracellular oxidation of non-fluorescent dye $H_2$-DCFDA. In the presence of ROS, $H_2$-DCFDA is oxidized to form green fluorescent dichlorofluoroscein (DCF) upon excitation at 485 nm. The extent of ROS production in the

treated cell was measured by percentage of cells with increased fluorescence intensity in comparison to untreated control cells. It was observed that fluorescence intensity (**Fig. 4A)** in the treated cells was significantly less compared to the untreated cells though reverse was expected. Kumar *et al*. [28] investigated the antimicrobial activity of AgNPs against freshwater isolated bacterial stain *Bacillus thuringiensis*, *Bacillus aquimaris* and their consortium. A significant amount of ROS generation was recorded in nanoparticles (NPs) treated individual isolates as well as in the consortium. They observed that fluorescence intensity of DCF was much higher in treated cells compared to the control. The generation of ROS caused oxidative injury in the cell causing disruption of the bacterial cell membrane integrity. Nel *et al*. [29] also evaluated ROS generation in the cells after treatment with NPs. They proposed that NPs treatment disturbed the equilibrium between the oxidant and antioxidant processes, which caused intracellular oxidative stress leading NPs mediated toxicity in the cells. On the contrary, **Fig. 4B-C** of the present study showed that fluorescence intensities of DCF in the treated cells were reduced with increase in concentration of NSAgNC as well as exposure time. This clearly indicates that ROS was not generated in the treated cells. Rather, the concentration and time dependent decrease in fluorescent intensities indicated that ROS production was inhibited in NSAgNC treated cells. Decomposition of hydrogen peroxide by NSAgNC and/ or scavenging of free radicals might be responsible for inhibition of ROS production in the treated cells. Recently, Menchón *et al.* [30] also reported that $Au/CeO_2$ nanoparticles inhibited the production of ROS through decomposition of hydrogen peroxide and protect the cells from oxidative stress.

The oxidative stress in the treated cells was further tested through measurement of intracellular concentration of GSH, which is a three-residue thiol-containing polypeptide. It is present at high levels (1−10 mM) in most of the gram-negative bacteria and maintains the cellular redox environment and protecting the cells against oxidative stress [31]. The GSH is predominantly present in reduced form in the cells; however, spontaneously oxidize upon exposure to the molecular oxygen ($O_2$ + 2R-SH → RSSR + $H_2O_2$; $\Delta G_0$= − 96 kJ/mol) [32]. Significant oxidation of GSH into its disulfide (GSSG) is leading to the cell death. Therefore, *in vitro* determination of GSH concentration is also an indicator to measure the cellular oxidative stress. The intracellular GSH concentration determination showed that GSH concentration in NSAgNC treated cells remained same to that of the untreated cells. The control *E. coli* and *P. aeruginosa* contained 8.9 ±1.2 and 7.1 ± 0.8 mM, respectively of GSH and in the treated (2.0 mg/mL of NSAgNC) cells it was found to be 8.4 ±1.2 and 6.5 ± 0.8 mM, respectively. Thus, GSH concentration in both treated and untreated cells was sufficient to scavenge the ROS and protect the cells from oxidative injury.

The viability of the NSAgNC treated cells was further tested using LIVE/DEAD viability assay containing DNA-binding fluorescent dyes SYTO 9 (green) and propidium iodide (red). SYTO 9 is permeable in both live and dead bacteria and stain green fluorescent color. On the other hand, propidium

iodide is penetrated only into the compromised cells owing to their altered membrane potential and exhibits red fluorescence. This simultaneously diminishes the fluorescence properties of SYTO 9. Live bacteria therefore strain green color, while dead bacteria exhibit strong red emission. The untreated *E. coli* and *P. aeruginosa* (**Fig. 4D, F**) showed living and healthy cells with green fluorescence. A significant decrease in cell viability was observed after exposure of the cells to NSAgNC. Populations of the compromised or dead cells increased with increase in concentration of NSAgNC. *E. coli* and *P. aeruginosa* following treatment with 2.0 mg/mL of NSAgNC (**Fig. 4E, G**) showed completely dead red cells. This observation suggested that NSAgNC caused damage to the bacterial cell membrane, altered the membrane permeability and ultimately leading to the cell death. Since, ROS and GSH assays established that intracellular GSH concentration was enough to scavenge the ROS production and protected the cells from oxidative damage; the cell viability assay clearly demonstrated that antibacterial activity of NSAgNC against gram-negative bacteria *E. coli* and *P. aeruginosa* occurred through ROS independent pathway. Recently, few reports also demonstrated ROS independent antibacterial activity of NPs [33,34]. Leung *et al*. [33] proposed the ROS independent antibacterial activity of MgO NPs against *E. coli*. The intracellular ROS generation was estimated through electron spin resonance study and proteomic analysis demonstrating that MgO NPs exhibited robust antibacterial activity in absence ROS production and without inhibition of lipid peroxidation activity. The binding of MgO NPs on the cell wall caused physical damage to the cell membrane and compromised cell membrane was a major factor for the cell death. Cui *et al*. [34] also revealed through transcriptomic and proteomic analysis that antibacterial activity of gold NPs occurred in absence ROS production. They observed that binding of gold NPs altered the membrane potential, which inhibited ATP synthesis and subsequently reduced the energy metabolism of the cells. In addition, the transcription of the cells was also inhibited through inhibition of binding of ribosomal subunit to tRNA. Our experimental results therefore, very consistent with the reported results of Leung *et al*. [33] and Cui *et al*. [34] for ROS independent antibacterial activity of metal nanoparticles.

### *3.4. Particle specific antibacterial activity*

There is a long standing debate regarding antibacterial mechanism of AgNPs. It has been reported that under environmental condition $Ag^+$ ions are leached out from AgNPs [26,27] and bind with the cell surface proteins through sulphur groups and inhibited the bacterial growth [21]. However, few reports demonstrated that the antibacterial activity of AgNPs is not solely due to released $Ag^+$ ions, rather, it depends on size, shape, surface charge, and solution chemistry of AgNPs [21,35,36]. In order to further establish the mechanism of action, the antibacterial activity of NSAgNC was performed under strictly anaerobic condition to eliminate the possibility of $Ag^+$ ion leaching by aerial oxidation [37]. Results (Supporting data **Fig. S2)** showed that under anaerobic condition NSAgNC demonstrated antibacterial

activity on *E. coli* and *P. aeruginosa* similar to that of aerobic condition. The leaching of $Ag^+$ ions was also not detected by AAS analysis under the experimental condition. We therefore, confirm that the dose response antibacterial activity of NSAgNC is solely due to "particle-specific" effect not by leaching of $Ag^+$ ions. For further confirmation, TEM images of the bacterial cells were recorded, which showed loss of *E. coli* (**Fig. 5A**) and *P. aeruginosa* (**Fig. 5B**) cellular integrity after exposure to 2.0 mg/mL of NSAgNC for 5 h. The binding of electron dense nanomaterials on the bacterial cell wall was clearly evident in the images and confirmed as NSAgNC through EDXA spectra (**Fig. 5C**). The membranes of the treated cells were roughed and damaged severely; lesions and holes were observed on the cell surface (indicated by arrow in the figures), indicating irreversible cell death, which is consistent with our previous observations [14]. Fragmentation of the cells was also noticed after interaction with NSAgNC. The extensive damage of the cell membrane and loss of cellular integrity structure suggested that NSAgNC not only perturb the cell membrane but also chemically degrade or oxidize the cell wall. The formation of holes or lesions as well as fragmentation of cells caused to leakage of cytoplasmic contents and this was confirmed through membrane destabilization assay (see supporting data). Supporting data **Table S2** showed the protein concentration in the extracellular region after treatment of *E. coli* and *P. aeruginosa* with NSAgNC. The untreated cells were served as control. Results clearly demonstrated that extracellular protein concentrations were much higher in NSAgNC treated cells compared to untreated cells and the protein concentration increased with increase in NSAgNC concentration. For example, extracellular protein concentration in the untreated *E. coli* was 0.2 ± 0.05 mg/mL, while protein concentration increased to 1.2 ± 0.4 mg/mL when the cells were treated with 2 mg/mL of NSAgNC. Hence, the direct interaction of NSAgNC with bacterial cells caused destabilization of membrane, leading to leakage of cytoplasmic protein into extracellular region. This led to increase in protein concentration in the extracellular region of the treated cells. Silver has high redox potential [$E_H°(Ag+/Ag°)$ = 0.8 V], therefore, the surface binding of NSAgNC could cause oxidative decomposition of the cell wall including surface proteins and lipopolysaccharide molecules [14]. The surface binding and effect of surface charge of NSAgNC on antibacterial activity was further studied using pH conditioned NSAgNC against *E. coli*. Prior to this experiment, NSAgNC was conditioned at different pH values (2.0−10.0) followed by washing with double distilled water to remove excess $H^+$ or $OH^-$ ions and antibacterial activity of NSAgNC was then conducted as described in the previous section. This pH conditioning altered the surface charge of NSAgNC. The experimental data demonstrated that NSAgNC conditioned at pH values <7.0 (Supporting data **Table S3**) exhibited higher antibacterial activity; with subsequent increase in pH values the antibacterial efficiency was reduced. At pH values <7.0 the positive charge of NSAgNC favored the electrostatic binding of NSAgNC to the negatively charged bacterial cell surfaces (-9.6 ± 0.7 mV zeta potential), which led to membrane disruption resulted in significant bactericidal effect. However, other mode of binding of NSAgNC on the cell surface could not be ruled out. Apart from electrostatic

interaction, binding of NSAgNC on the cell wall might occur through van der Waals interaction, covalent binding through soft acid base interaction and physical adsorption to contribute in the antimicrobial mechanism, since NSAgNC also exhibited considerable antibacterial activity at higher pH values. Most importantly, the initial binding of NSAgNC on the cell wall promote their interaction with cell surface inducing physical damage to the cell membrane and finally leading to the cell death through release of intracellular materials.

### *3.5. Inhibition of respiratory chain enzyme and metabolic arrest*

To comprehend the mechanism of "particle-specific" antibacterial activity, the effect of NSAgNC on respiratory chain enzyme dehydrogenase and cellular metabolic activity were studied. The enzymatic activity of dehydrogenase was determined by conversion of colorless iodonitrotetrazolium chloride (INT) to water insoluble and dark red iodonitrotetrazolium formazan (INF) by the bacterial respiratory chain dehydrogenase [38]. The effect of NSAgNC on dehydrogenase activity was shown in supporting data **Fig. S3A**. The untreated cells converted colorless INT to red color INF exhibiting dehydrogenase activity, while the treated cells exhibited variable enzymatic activity. Cells when treated with low concentrations of NSAgNC (<0.25 mg/mL) could able to convert INT to INF and demonstrated considerable dehydrogenase activity; however with increase in concentration of NSAgNC as well as exposure time the dehydrogenase activity was reduced. The cells after being treated with 1.5 mg/mL of NSAgNC for 8 h did not exhibit any dehydrogenase activity and unable to convert INT to INF. The results thus, indicated that dehydrogenase activity was inhibited by NSAgNC. It is therefore, proposed that NSAgNC destroyed respiratory chain dehydrogenase following their internalization through damaged cell membrane and inhibiting respiration of cells. Kim *et al.* [39] earlier reported that $Ag^+$ ions form –S–Ag following interaction with thiol (–SH) group of proteins and hindering the enzymatic function, leading to inhibition of *E. coli* growth.

In consistent with this result, the metabolic activity of the cells was further assayed by Alamar Blue method based on the reduction of the purple, non-fluorescent dye resazurin (Alamar Blue) to the pink, fluorescent dye resorufin by living cells. The reduction rate of resazurin to resorufin is proportional to the metabolic activity and number of living cells. It was clearly observed that purple color of Alamar Blue was turned to pink by untreated cells (Supporting data **Fig. S3B, inset**), however, the dead cells ($H_2O_2$ treated cells) unable to metabolize the Alamar Blue and remained purple. It was interesting to note that in NSAgNC treated cells, the reduction of Alamar Blue was dependent upon the concentration of NSAgNC (Supporting data **Fig. S3B**). At low concentration of NSAgNC, the reduction of resazurin to resorufin was noted; however, at higher concentration the cells unable to metabolize the Alamar Blue and remained purple. Thus metabolic activity of the cells was reduced with increasing the concentration of NSAgNC. Cells after being treated with NSAgNC at a concentration of >1.0 mg/mL, the reduction of resazurin to

resorufin was completely inhibited and cells become metabolically inactive. Treatment of bacterial cells with NSAgNC thus reduced the metabolic activity of the cells and inhibited the enzymatic activity of respiratory chain dehydrogenase leading to growth inhibition of the cells. It is well known that the outer cell membrane of gram-negative bacteria acts as a selective permeable barrier protecting the cells from harmful agents. The binding of NSAgNC on the outer cell membrane therefore, broke the membrane permeability barrier and subsequently deactivate the respiratory chain dehydrogenase following internalization of NSAgNC into intracellular region, and uncoupling the respiration from oxidative phosphorylation [40]. This led to depletion of intracellular ATP levels [41], which in turn caused metabolic arrest in the cells and affect the cell viability.

*3.6. DNA damage and protein synthesis inhibition*

Owing to the pore formation in the cell membrane, NSAgNC could be readily diffused into the nucleus and further accelerate DNA condensation or damage upon binding with DNA causing inhibition of replication and impairment of protein synthesis [38,42]. It is well known that replication of DNA occurs effectively in relaxed state, but loses the replication in condensed state. The possibility of DNA damage was studied through agarose gel electrophoresis analysis. Both plasmid and genomic DNA were extracted from cells before and after treatment with NSAgNC and fragmentation of DNA was analyzed. The electrophoresis pattern clearly showed decrease in genomic (**Fig. 6A-B**) and plasmid (**Fig. 6C-D**) DNA band intensity in the treated cells in comparison to the control cells. Besides, eletrophoretic mobility of DNA was higher in the treated cells as compared to the untreated control cells. The length of DNA “laddering” pattern and decrease in band intensity indicated a non-specific and dose-dependent DNA damage by NSAgNC. An extensive DNA damage was noticed when cells were treated with 1.5 mg/mL or higher concentration of NSAgNC. The result of dose-dependent DNA damage was very consistent to that of cell viability loss. Due to the small size and high redox potential of silver, NSAgNC could easily penetrate through pore of the damaged cells and caused oxidative damage to the DNA upon binding with the DNA. On the other hand release of $Ag^+$ ions and subsequent binding to DNA causing DNA damage has also been suggested. Rai and Bai [43] proposed that $Ag^+$ ions released from AgNPs interacted with the phosphorous moieties in DNA leading to the inhibition of DNA replication. Since, we did not detect any leaching of $Ag^+$ ions, DNA damage related to $Ag^+$ ions binding may be ruled out. It has also been proposed that silver has affinity for guanine N7 and adenine N7 of DNA, leading to formation different types of Ag–DNA complex [44–46]. At lower ratio of Ag/nucleotide ($r<0.2$), type I complex is formed by binding of silver with N7 of guanine or adenine, whereas type II complex is formed when $r = 0.2–0.5$, where A-T or G-C base pairs is the main binding sites for silver. At $r>0.5$, type III complex is formed when the major binding sites in the type I and type II complexes are saturated. Dattagupta and Crotters [45] reported that type II complex of silver DNA induced the conformational change of DNA

from its B- form structure with propeller twisted base pairs to a structure of flat base pairs, and regains the B-form structure with formation of type II complex. Later, Arakawa *et al*. [46] demonstrated through FTIR and capillary electrophoresis studies that in type I silver–DNA complex, silver binds DNA at guanine N7 when r = 1/80, whereas at higher concentration silver binds to N7 of adenine. With further increase in ratios (r =1/2), type II complex is formed through binding of silver to both A-T and G-C base pairs without much change in the conformation of DNA. Therefore, binding of NSAgNC with DNA caused oxidative damage or condensation of DNA, which inhibited the replication of DNA and finally leading to the cell death.

The effect of NSAgNC treatment on cellular proteins expression was studied by proteomic analysis. The SDS–PAGE (Supporting data **Fig. S4**) of *E. coli* showed considerable change in the intracellular protein profile of NSAgNC treated cells compared to the untreated control cells. Following treatment with NSAgNC, down-regulation (Lane 3-7) of proteins was noticed. In treated samples few bands were missing and band intensities were also lowered compared to the control one (Lane 2). Similar result was also obtained in *P. aeruginosa* after treatment with NSAgNC (data not shown). The results thus showed that the protein expressions were suppressed by NSAgNC. The condensation and/ or damage of DNA due to interaction with NSAgNC inhibited the replication of DNA, which caused impairment of protein synthesis. In addition, binding of NSAgNC with cellular proteins may also damage the proteins. This caused down regulation of cellular metabolism and ATP synthesis inhibition [33,47-49]. Alteration in expression of different heat shock (IbpA, IbpB, and 30S ribosomal subunit S6) and envelop (i.e., OmpA, OmpC, OmpF, OppA, MetQ) proteins after short exposure of *E. coli* to AgNPs has been reported by Lok *et al*. [48]. The authors also demonstrated that binding of AgNPs destabilized the outer membrane of the cells, which altered the membrane potential and subsequently depleted the intracellular ATP levels. Very recently, Leung and co-workers [33] reported the down-regulation of outer membrane proteins such as channel porins and ion channel proteins as well as ribosomal and other cellular proteins in *E. coli* after exposure to MgO. Other reports [49,50] also demonstrated that AgNPs strongly bind to different enzymes and non-enzyme proteins including porins, chaperones, or periplasmic peptide-binding proteins and inhibiting their activities. In consistence with these results, we therefore, suggest that NSAgNC exhibited ROS independent “particle-specific” antibacterial activity through multiple steps (**Fig. 7**); as (i) in close proximity to the cells, the binding of NSAgNC on the cell surface damaged the cell membrane, (ii) destabilization of the cell membranes increased the membrane permeability, which subsequently induced the leakage of cellular materials, (iii) NSAgNC entered the inner membrane and inactivate respiratory chain dehydrogenases, and consequently uncoupling the respiration from oxidative phosphorylation and finally caused metabolic arrest in the cells, (iv) NSAgNC simultaneously decomposed the cell membrane due to high redox potential of silver, (v) NSAgNC bound with DNA and intracellular proteins upon

diffused into cytosol, resulting in DNA damage and down-regulation of protein expressions leading to the cell death.

## 4. Conclusions

Microbial protein mediated biosynthesis of NSAgNC has been demonstrated for disinfection of contaminated water. The NSAgNC exhibited long term antibacterial activity in a dose dependent manner on *E. coli* and *P. aeruginosa*. ~99.9% of these pathogenic bacteria were killed at a concentration of 1.5 mg/mL of NSAgNC within 5 h. Intracellular ROS production and dissociation of $Ag^+$ ions were not recorded in the antibacterial activity of NSAgNC. TEM observation along with experiments under anoxic condition demonstrated that NSAgNC explicit "particle-specific" antibacterial activity. Binding of NSAgNC on the bacterial cells surface resulted in membrane damage, which caused loss of the cell membrane integrity, alteration in membrane permeability and leakage of cytoplasmic materials. NSAgNC also inhibited respiratory chain dehydrogenase leading to uncoupling of oxidative phosphorylation, which further caused metabolic arrest in the cells. Genomic studies further demonstrated the fragmentations of DNA, whereas proteomic studies revealed alteration in proteins expression in the NSAgNC treated cells. Overall, NSAgNC exhibited robust "particle specific" antibacterial activity in absence of intracellular ROS production and dissolution of $Ag^+$ ions. Therefore, the biosynthesized NSAgNC can be used for environmental sustainable water purification.

## Acknowledgements

The authors acknowledge the Department of Science and Technology (DST), Government of India for research support under Fast Track Scheme (SR/FT/LS-80/2012) and Council of Scientific and Industrial Research (CSIR), Government of India for financial assistance under the STRAIT programme (CSIR-CLRI Communication No. 1126).

## Appendix A. Supplementary data

Supplementary data associated with this article can be found inthe online version.

## References

[1] U.S. EPA, Reducing Risk: Setting priorities and strategies for environmental protection. Appendix B: Report of the human health subcommittee; SAB-EC-90-021B, USEPA Science Advisory Board, Washington, 1990.
[2] Water for Life, Making it Happen (WHO, UNICEF, 2005).
[3] S.W. Krasner, H.S. Weinberg, S.D. Richardson, S.J. Pastor, R. Chinn, M.J. Sclimenti, G.D. Onstad, A.D. Thruston Jr., Environ. Sci. Technol. 40 (2006) 7175-7185.
[4] IWSA, The practice of chlorination: Application, efficacy, problems and alternatives, international water supply association blue pages, 1997.

[5] M.A. Shannon, P.W. Bohn, M. Elimelech, J.G. Georgiadis, B.J. Mariñas, A.M. Mayes, Science and technology for water purification in the coming decades, Nature 452 (2008) 301-310.

[6] S.K. Das, A.R. Das, A.K. Guha, Gold nanoparticles: microbial synthesis and application in water hygiene management, Langmuir 25 (2009) 8192–8199.

[7] A.K. Singh, P. Singh, S. Mishra, V.K. Shahi, Anti-biofouling organic-inorganic hybrid membrane for water treatment, J. Mater. Chem. 22 (2012) 1834–1844.

[8] P. Gunawan, C. Guan, X.H. Song, Q.Y. Zhang, S.S.J. Leong, C.Y. Tang, Y. Chen, M.B. Chan-Park, M.W. Chang, K.A. Wang, R. Xu, Hollow fiber membrane decorated with Ag/MWNTs: Toward effective water disinfection and biofouling control, ACS Nano 5 (2011) 10033–10040.

[9] H. Zhang, V. Oyanedel-Craver, Comparison of the bacterial removal performance of silver nanoparticles and a polymer based quaternary amine functiaonalized silsesquioxane coated point-of-use ceramic water filters, J. Hazard. Mater. 260 (2013) 272–277.

[10] C. Levard, E.M. Hotze, G.V. Lowry, G.E. Brown, Jr., Environmental transformations of silver nanoparticles: Impact on stability and toxicity, Environ. Sci. Technol. 46 (2012) 6900−6914.

[11] R.J. White, R. Luque, V.L. Budarin, J.H. Clark, D.J. Macquarrie, Supported metal nanoparticles on porous materials. Methods and applications, Chem. Soc. Rev. 38 (2009) 481–494.

[12] J.A. Dahl, B.L.S. Maddux, J.E. Hutchison, Toward greener nanosynthesis, Chem. Rev. 107 (2007) 2228–2269.

[13] D.P. Tamboli, D.S. Lee, Mechanistic antimicrobial approach of extracellularly synthesized silver nanoparticles against gram positive and gram negative bacteria, J. Hazard. Mater. 260 (2013) 878–884.

[14] S.K. Das, M.M.R. Khan, A.K. Guha, A.R. Das, A.B. Mandal, Silver-nanobiohybride material: Synthesis, characterization and application in water purification, Bioresour. Technol. 124 (2012) 495–499.

[15] N. Jain, A. Bhargava, S. Majumdar, J.C. Tarafdar, J. Panwar, Extracellular biosynthesis and characterization of silver nanoparticles using *Aspergillus flavus* NJP08: A mechanism perspective, Nanoscale 3 (2011) 635-641.

[16] S.K. Das, M.M.R. Khan, A.K. Guha, N. Naskar, Bio-inspired fabrication of silver nanoparticles on nanostructured silica: characterization and application as a highly efficient hydrogenation catalyst, Green Chem. 15 (2013) 2548–2557.

[17] S. Chernousova, M. Epple, Silver as antibacterial agent: Ion, nanoparticle, and metal, Angew. Chem. Int. Ed. 52 (2013) 1636–1653.

[18] E. Amato, Y.A. Diaz-Fernandez, A. Taglietti, P. Pallavicini, L. Pasotti, L. Cucca, C. Milanese, P. Grisoli, C. Dacarro, J.M. Fernandez-Hechavarria, V. Necchi, Synthesis, characterization and antibacterial activity against gram positive and gram negative bacteria of biomimetically coated silver nanoparticles, Langmuir 27 (2011) 9165–9173.

[19] S. Kittle, C. Greulich, J. Diendorf, M. Köller, M. Epple, Toxicity of silver nanoparticles increases during storage because of slow dissolution under release of silver ions, Chem. Mater. 22 (2010) 4548–4554.

[20] O. Bondarenko, A. Ivask, A. Käkinen, I. Kurvet, A. Kahru, Particle-cell contact enhances antibacterial activity of silver nanoparticles, PLoS ONE 8 (2013) e64060.

[21] L. Rizzello, P. P. Pompa, Nanosilver-based antibacterial drugs and devices: Mechanisms, methodological drawbacks, and guidelines, Chem. Soc. Rev. 43 (2014) 1501–1518.

[22] J.S. Kim, E. Kuk, K.N. Yu, J.-H. Kim, S.J. Park, H.J. Lee, S.H. Kim, Y.K. Park, Y.H. Park, C.-Y. Hwang, Y.K. Kim, Y.S. Lee, D.H. Jeong, M.H. Cho, Antimicrobial effects of silver nanoparticles, Nanomed. Nanotechnol. 3 (2007) 95–101.

[23] W. Zhang, Y. Li, J. Niu, Y. Chen, Photogeneration of reactive oxygen species on uncoated silver, gold, nickel, and silicon nanoparticles and their antibacterial effects, Langmuir 29 (2013) 4647–4651.

[24] S.K. Das, M.M.R. Khan, T. Parandhaman, F. Laffir, A.K. Guha, G. Sekaran and A.B. Mandal, Nano-silica fabricated with silver nanoparticles: antifouling adsorbent for efficient dye removal, effective water disinfection and biofouling control, Nanoscale 5 (2013) 5549–5560.

[25] J. Sambrook, D.W. Russell, Molecular cloning; a laboratory manual, 3rd ed. Cold Spring Harbor Press: New York, 2001, Vol. 1.

[26] L. Xuan, J.J. Lenhart, H.W. Walker, Aggregation kinetics and dissolution of coated silver nanoparticles, Langmuir 28 (2012) 1095−1104.

[27] A.P. Gondikas, A. Morris, B.C. Reinsch, S.M. Marinakos, G.V. Lowry, H. Hsu-Kim, Cysteine-induced modifications of zero-valent silver nanomaterials: Implications for particle surface chemistry, aggregation, dissolution, and silver speciation, Environ. Sci. Technol. 46 (2012) 7037−7045.

[28] D. Kumar, J. Kumari, S. Pakrashi, S. Dalai, A.M. Raichur, T.P. Sastry, A.B. Mandal, N. Chandrasekaran, A. Mukherjee, Qualitative toxicity assessment of AgNPs on the fresh water bacterial isolates and consortium at low level of exposure concentration, Ecotox. Environ. Safe. 108 (2014) 152–160.

[29] A. Nel, T. Xia, L. Mädler, N. Li, Toxic potential of materials at the nanolevel. Sci. 311 (2006) 622–627.

[30] C. Menchón, R. Martín, N. Apostolova, V.M. Victor, M. Álvaro, J.R. Herance, H. García, Gold nanoparticles supported on nanoparticulate ceria as a powerful agent against intracellular oxidative stress, Small 8 (2012) 1895–1903.

[31] C.D. Vecitis, K.R. Zodrow, S. Kang, M. Elimelech, Electronic-structure-dependent bacterial cytotoxicity of single-walled carbon nanotubes, ACS Nano 4 (2010) 5471–5479.

[32] C.C. Winterbourn, D. Metodiewa, Reactivity of biologically important thiol compounds with superoxide and hydrogen peroxide, Free Radic. Biol. Med. 27 (1999) 322–328.

[33] Y.H. Leung, A.M.C. Ng, X. Xu, Z. Shen, L.A. Gethings, M.T. Wong, C.M.N. Chan, M.Y. Guo, Y.H. Ng, A.B. Djurišić, P.K.H. Lee, W.K. Chan, L.H. Yu, D.L. Phillips, A.P.Y. Ma, F.C.C. Leung, Mechanisms of antibacterial activity of MgO: Non-ROS mediated toxicity of MgO nanoparticles towards *Escherichia coli,* Small 10 (2013) 1171–1183.

[34] Y. Cui, Y. Zhao, Y. Tian, W. Zhang, X. Lü, X. Jiang, The molecular mechanism of action of bactericidal gold nanoparticles on *Escherichia coli*, Biomaterials 33 (2012) 2327–2333.

[35] A.M. El Badawy, R.G. Silva, B. Morris, K.G. Scheckel, M.T. Suidan, T.M. Tolaymat, Surface charge-dependent toxicity of silver nanoparticles, Environ. Sci. Technol. 45 (2011) 283–287.

[36] A. Panáček, L. Kvítek, R. Prucek, M. Kolář, R. Večeřová, N. Pizúrová, V.K. Sharma, T. Nevěčná, R. Zbořil, Silver colloid nanoparticles: synthesis, characterization, and their antibacterial activity, J. Phys. Chem. B 110 (2006) 16248–16253.

[37] Z.M. Xiu, Q.B. Zhang, H.L. Puppala, V.L. Colvin, P.J.J. Alvarez., Negligible particle-specific antibacterial activity of silver nanoparticles, Nano Lett. 12 (2012) 4271–4275.

[38] P. Sanpui, A. Chattopadhyay, S.S. Ghosh, Induction of apoptosis in cancer cells at low silver nanoparticle concentrations using chitosan nanocarrier, ACS Appl. Mater. Interfaces 3 (2011) 218–228.

[39] K.J. Kim, W.S. Sung, S.K. Moon, J.S. Choi, J.G. Kim, D.G. Lee, Antifungal effect of silver nanoparticles on dermatophytes, J. Microbiol. Biotechnol. 18 (2008) 1482–1484.

[40] K.B. Holt, A.J. Bard, Interaction of silver(I) ions with the respiratory chain of *Escherichia coli*: An electrochemical and scanning electrochemical microscopy study of the antimicrobial mechanism of micromolar $Ag^{+}$, Biochemistry 44 (2005) 13214–13223.

[41] S. Shrivastava, T. Bera, A. Roy, G. Singh, P. Ramachandrarao, D. Dash, Characterization of enhanced antibacterial effects of novel silver nanoparticles, Nanotechnology 18 (2007) 25103–225111.

[42] K. Li, X. Zhao, B.K. Hammer, S. Du, Y. Chen, Nanoparticles inhibit DNA replication by binding to DNA: Modeling and experimental validation, ACS Nano 7 (2013) 9664–9674.

[43] R.V. Rai, J.A. Bai, Nanoparticles and their potential application as antimicrobials. Science against microbial pathogens: communicating current research and technological advances. A. Méndez-Vilas (Ed.), 2011, 197-209.

[44] R.M. Izatt, J.J. Christensen, J.H. Rytting, Sites and thermodynamic quantities associated with proton and metal ion interaction with ribonucleic acid, deoxyribonucleic acid, and their constituent bases, nucleosides, and nucleotides, Chem Rev. 71 (1971) 439–481.

[45] N. Dattagupta, D.M. Crothers, Solution structural studies of the Ag(I)-DNA complex, Nucleic Acids Res. 9 (1981) 2971–2985.

[46] H. Arakawa, J.F. Neault, H.A. Tajmir-Riahi, Silver(I) complexes with DNA and RNA studied by Fourier transform infrared spectroscopy and capillary electrophoresis, J. Biophys. 81 (2001) 1580–1587.

[47] S.M. Ouda, Some nanoparticles effects on *Proteus* sp. and *Klebsiella* sp. isolated from water, Am. J. Infect. Dis. Microbiol. 2 (2014) 4–10.

[48] C.N. Lok, C.M. Ho, R. Chen, Q.Y. He, W.Y. Yu, H.Z. Sun, P.K.H. Tam, J.F. Chiu, C.M. Che, Proteomic analysis of the mode of antibacterial action of silver nanoparticles, J. Proteome Res. 5 (2006) 916–924.

[49] N.S. Wigginton, A. Titta, F. Piccapietra, J. Dobias, V.J. Nesatyy, M.J.F. Suter, R. Bernier-Latman, Binding of silver nanoparticles to bacterial proteins depends on surface modifications and inhibits enzymatic activity, Environ. Sci. Technol. 44 (2010) 2163–2168.

[50] C. Vannini, G. Domingo, E. Onelli, B. Prinsi, M. Marsoni, L. Espen, M. Bracale, Morphological and proteomic responses of *Eruca sativa* exposed to silver nanoparticles or silver nitrate, PLoS ONE 8 (2013) e68752.

**Ligend to Figures**

**Figure 1.** UV-vis spectrum (A), TEM image (B), and Zetal potential (C) of biosynthesized NSAgNC. Data represent an average of five independent experiments ± SD shown by error bar.

**Figure 2.** Antibaterial activity of NSAgNC against *E. coli* (A) and *P. aeruginosa* (C) by tubidity assay; Bacterial growth curves of *E. coli* (B) and *P. aeruginosa* (D) in NB media containing different concentration of NSAgNC demonstraing dose dependent antibacterial activity of NSAgNC; 1-8 corresponds negative control, 0.1 mg/mL, 0.25 mg/mL, 0.5 mg/mL, 1.0 mg/mL, 1.5 mg/mL, 2.0 mg/mL NSAgNC in the media and uninoculated media, respectively. Data represent an average of five independent experiments.

**Figure 3.** Killing efficiency of NSAgNC measured by plate count (A) and MTT (B) assay; killing kinetics of NSAgNC measured by MTT assay (C) showing time dependent antibacterial activity of NSAgNC. Data represent an average of five independent experiments ± SD shown by error bar.

**Figure 4**. Fluorescence intensity (A) of untreated and NSAgNC treated cells following staining with $H_2$-DCFDA; Effect of concentration of NSAgNC (B) and exposure time (C) on fluorescence intensity of treated cells; Viability of (D-E) *E. coli* and (F-G) *P. aeruginosa* cells after treatment with NSAgNC followed by staining with LIVE/DEAD assay kit. The images were recorded at 100× magnification using a fluorescence microscope. Data represent an average of five independent experiments ± SD shown by error bar.

**Figure 5**. Transmission electron microscopic images of *E. coli* (A) and *P. aeruginosa*(B) following treatment with 2 mg/mL of NSAgNC for 5 h; EDXA spectrum (C) of the treated cells. Arrows indicate pore formation on the cells, whereas marked areas indicate EDXA spectral regions.

**Figure 6.** Electrophoresis analysis of genomic (A, C) and plasmid (B, D) DNA of *E. coli* and *P. aeruginosa* following treatment with different concentration of NSAgNC for 5 h.

**Figure 7.** Schematic presentation of mechanistic aspect of “particle-specific” antibacterial activity of NSAgNC.

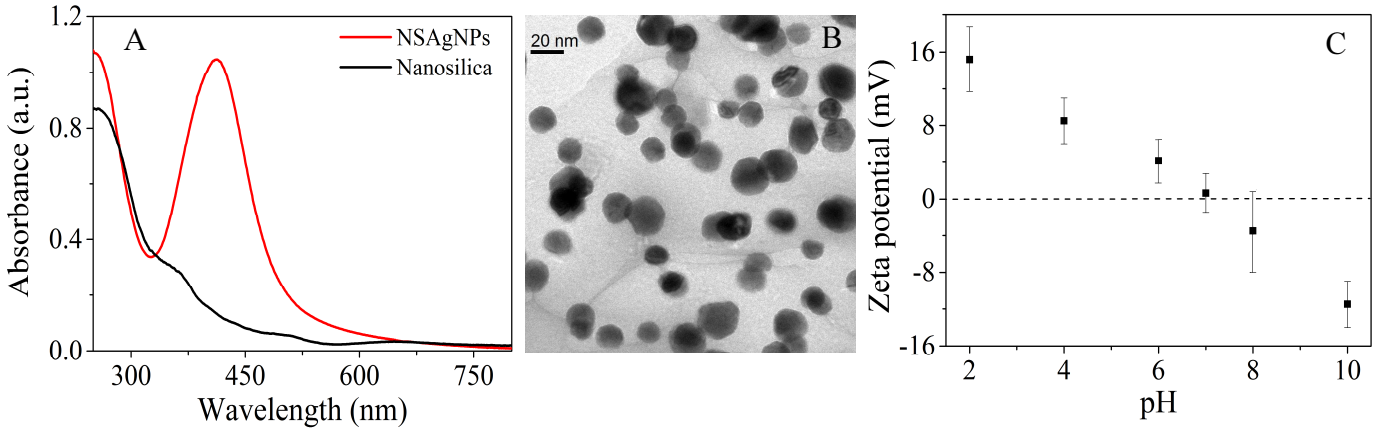
A
NSAgNPs
Nanosilica
Absorbance (a.u.)
Wavelength (nm)
1.2
0.8
0.4
0.0
300
450
600
750
20 nm
B
C
Zeta potential (mV)
pH
16
8
0
-8
-16
2
4
6
8
10

**Fig. 1**

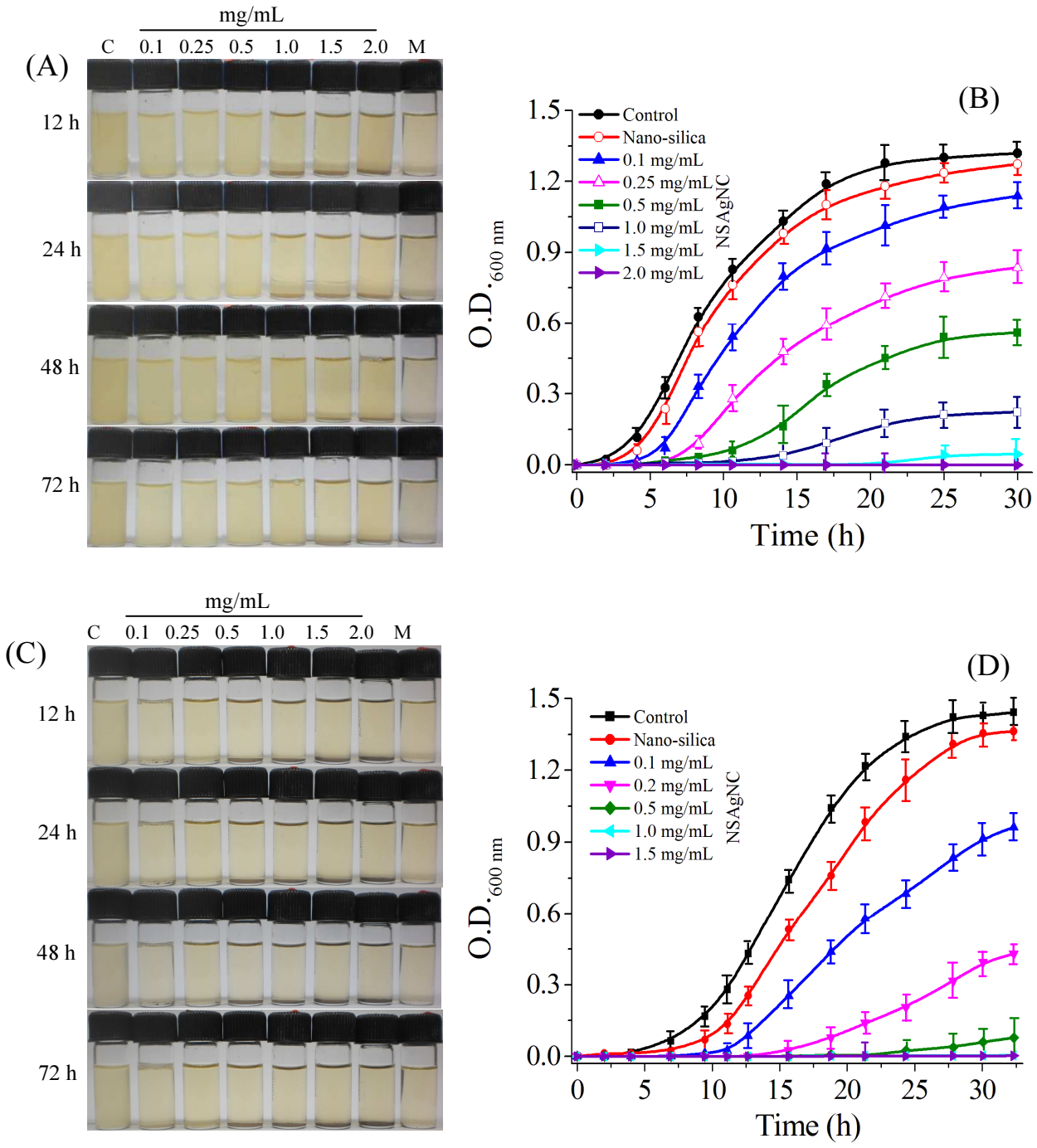
(A)
mg/mL
C 0.1 0.25 0.5 1.0 1.5 2.0 M
12 h
24 h
48 h
72 h
(B)
Control
Nano-silica
0.1 mg/mL
0.25 mg/mL
0.5 mg/mL
1.0 mg/mL
1.5 mg/mL
2.0 mg/mL
NSAgNC
O.D.600 nm
Time (h)
(C)
mg/mL
C 0.1 0.25 0.5 1.0 1.5 2.0 M
12 h
24 h
48 h
72 h
(D)
Control
Nano-silica
0.1 mg/mL
0.2 mg/mL
0.5 mg/mL
1.0 mg/mL
1.5 mg/mL
NSAgNC
O.D.600 nm
Time (h)

**Fig. 2**

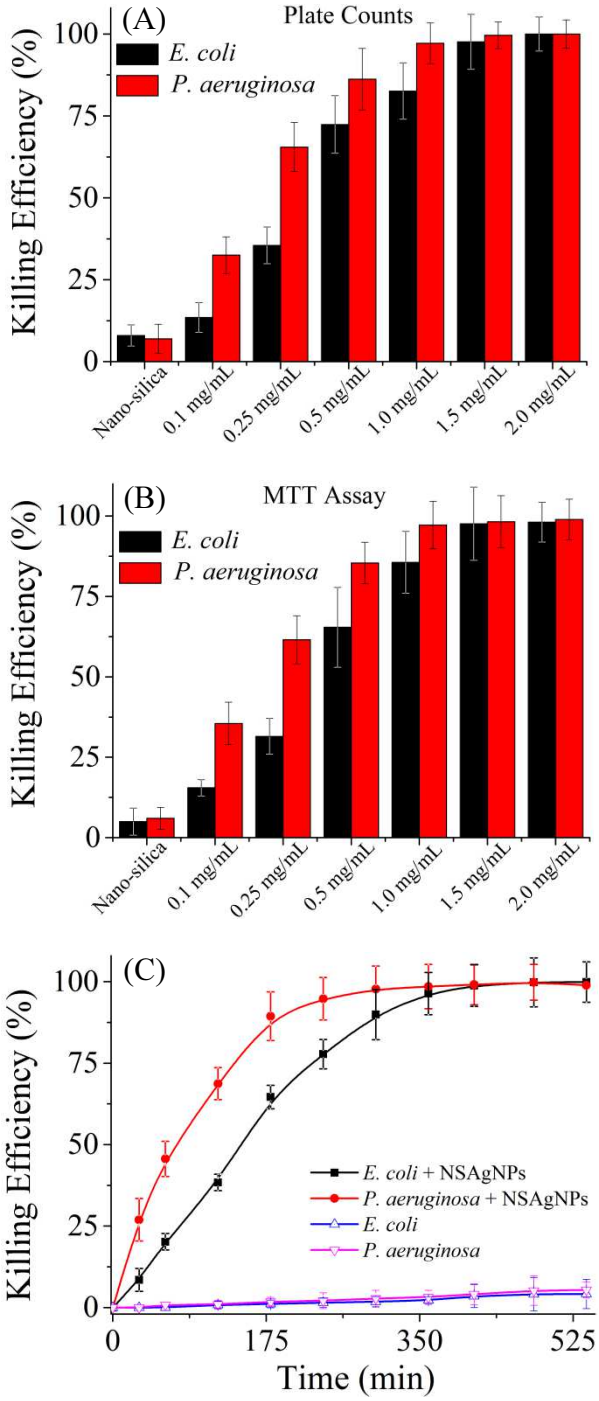
(A)
Plate Counts
E. coli
P. aeruginosa
Killing Efficiency (%)
100
75
50
25
0
Nano-silica
0.1 mg/mL
0.25 mg/mL
0.5 mg/mL
1.0 mg/mL
1.5 mg/mL
2.0 mg/mL
(B)
MTT Assay
E. coli
P. aeruginosa
Killing Efficiency (%)
(C)
E. coli + NSAgNPs
P. aeruginosa + NSAgNPs
E. coli
P. aeruginosa
0
175
350
525
Time (min)

**Fig. 3**

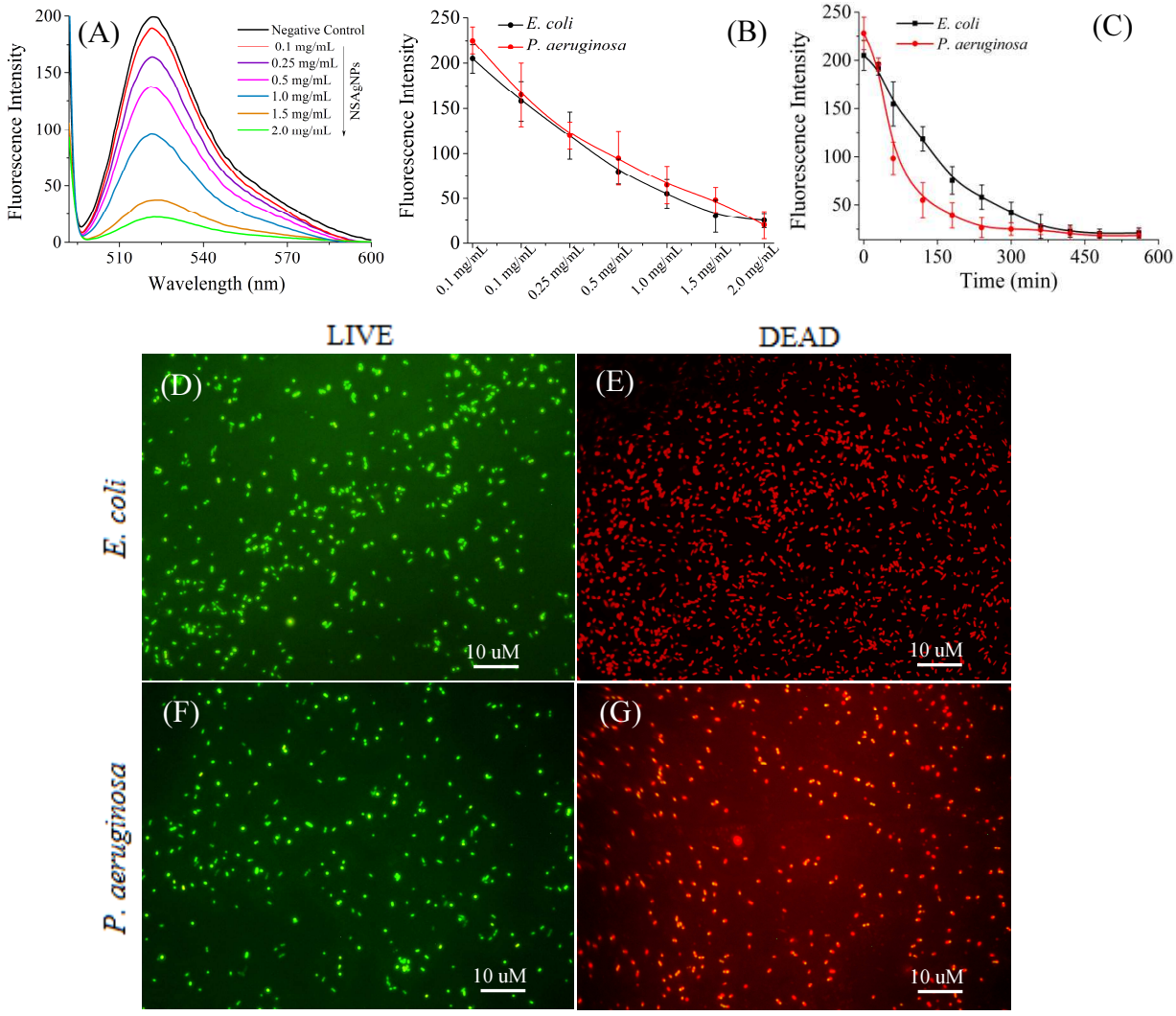
(A)
Fluorescence Intensity
Wavelength (nm)
Negative Control
0.1 mg/mL
0.25 mg/mL
0.5 mg/mL
1.0 mg/mL
1.5 mg/mL
2.0 mg/mL
NSAgNPs
(B)
E. coli
P. aeruginosa
Fluorescence Intensity
0.1 mg/mL
0.1 mg/mL
0.25 mg/mL
0.5 mg/mL
1.0 mg/mL
1.5 mg/mL
2.0 mg/mL
(C)
E. coli
P. aeruginosa
Fluorescence Intensity
Time (min)
LIVE
DEAD
(D)
(E)
(F)
(G)
E. coli
P. aeruginosa
10 uM

**Fig. 4**

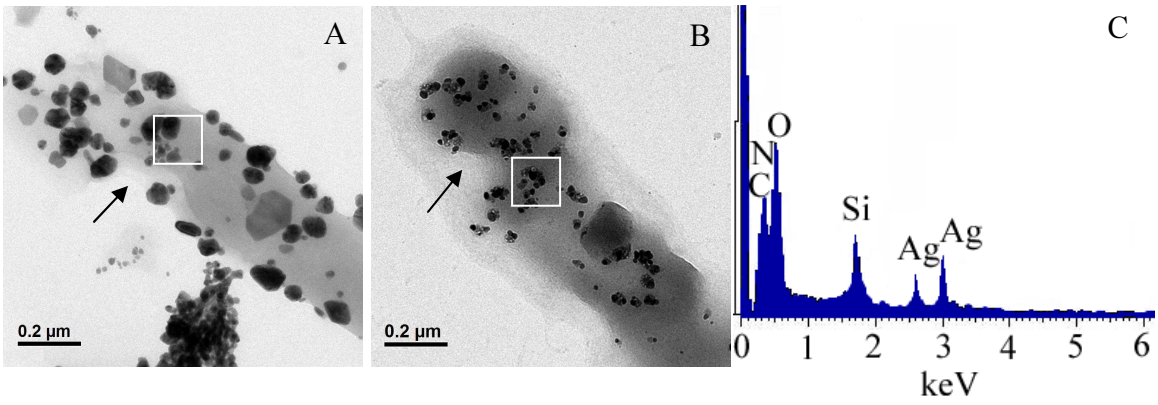


**Fig. 5**

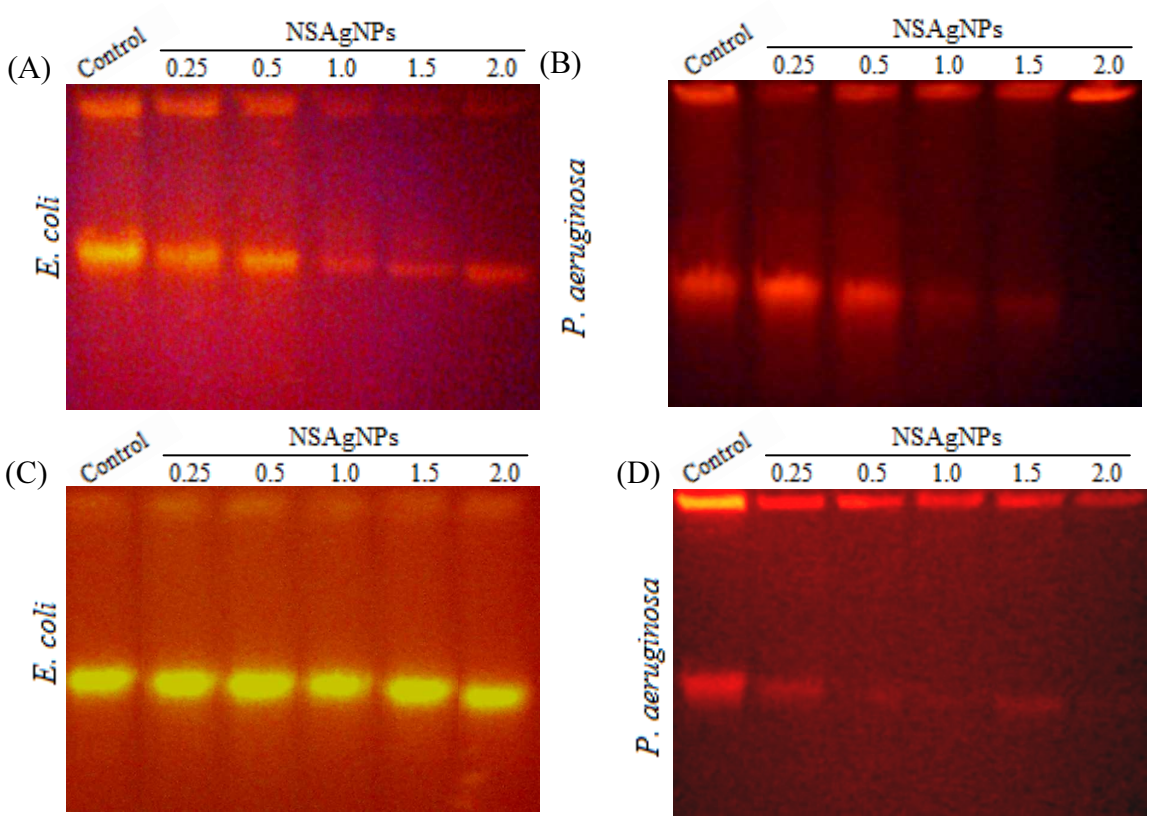
(A)
Control
NSAgNPs
0.25
0.5
1.0
1.5
2.0
E. coli
(B)
Control
NSAgNPs
0.25
0.5
1.0
1.5
2.0
P. aeruginosa
(C)
Control
NSAgNPs
0.25
0.5
1.0
1.5
2.0
E. coli
(D)
Control
NSAgNPs
0.25
0.5
1.0
1.5
2.0
P. aeruginosa

**Fig. 6**

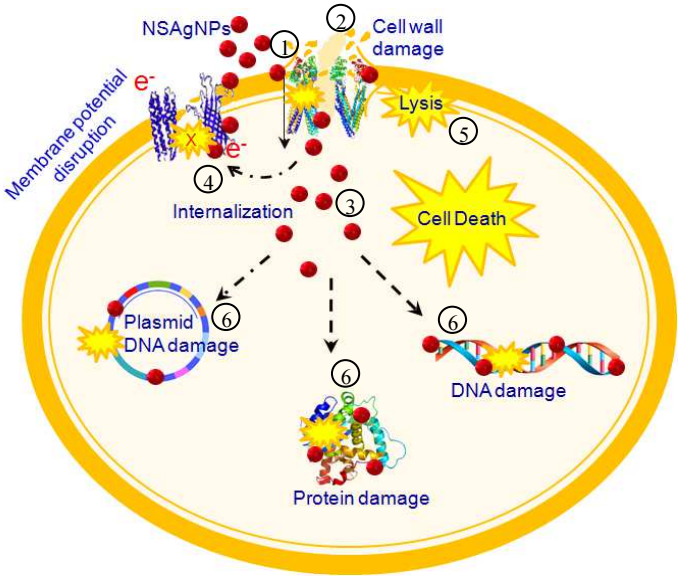
NSAgNPs
1
2
Cell wall damage
Membrane potential disruption
e-
e-
X
Lysis
5
4
Internalization
3
Cell Death
Plasmid DNA damage
6
6
6
DNA damage
Protein damage

**Fig. 7**

## Supporting Information

# Antimicrobial Behavior of Biosynthesized Silica-Silver Nanocomposite for Water Disinfection: A Mechanistic Perspective

Thanusu Parandhaman[a,d,≠], Anisha Das[a,≠], B. Ramalingam[a], Debasis Samanta[b], T. P. Sastry[a], Asit Baran Mandal[c,d*] and Sujoy K. Das[a,d*]

[a]Bioproducts Laboratory, [b]Polymer Division, and [c]Chemical Laboratory, Council of Scientific and Industrial Research (CSIR)–Central leather Research Institute (CLRI), Chennai– 600020, India, and [d]Academy of Scientific and Innovative Research (AcSIR), New Delhi– 110001, India.
[≠]Both the authors have equal contribution

### Experimental Methods

*Microorganisms*

*Rhizopus oryzae* (NCIM 1009), *Escherichia coli* (MTCC 062), and *Pseudomonas aeruginosa* (MTCC 424) were obtained from the Institute of Microbial Technology, Chandigarh, India, and were maintained on potato dextrose (2% potato extract, 2% dextrose, and 1.5% Agar) and nutrient (5% beef extract, 3% peptone, and 1.5% agar) agar slants, respectively.

*Synthesis of NSAgNC*

Protein mediated synthesis of silver nanoparticles on nanostructured silica was carried out as follows. 200 mL of 5 mM $AgNO_3$ solution was added to 5 g of nano-silica powder and incubated with shaking (120 rpm) at 30 °C for 5 h. 25 mL protein extract (6 mg/mL) of *R. oryzae* was then added to the solution and incubated at 30 °C for another 48 h with shaking. Following incubation, the material was separated by centrifugation (10,000 rpm, 15 min), washed thoroughly with deionized and double distilled water and finally dried at 50 °C in a hot air oven. The as-prepared NSAgNC was characterized through UV-vis spectroscopy and transmission electron microscopy.

*Spread plate method*

The microbicidal activities of NSAgNC on these organisms were determined by plate count method. In brief, 3 mL bacterial cells ($10^7$ CFU/mL) were treated with NSAgNC (0–2.0 mg/mL) for different time intervals under shaking (120 rpm) conditions. Aliquots were taken out at different incubation period and spread over the nutrient agar plates with appropriate dilutions. The plates were then incubated at 37 °C overnight and the number colonies were counted.

*Antibacterial activity under anaerobic condition*

The antibacterial activity of NSAgNC was repeated under anaerobic condition keeping other parameters same to determine the effect of $Ag^+$ ions leached out from NSAgNC. The dispersed solution of NSAgNC was taken in sealed test tubes. $N_2$ gas was then purged in the test tubes to fully remove the oxygen and incubated for 5 h. A freshly grown *E. coli* and *P. aeruginosa* culture were then injected into the test tubes separately and incubated for 10 h under anaerobic condition. At different time intervals cells were collected through sterile syringe and number of viable cells was counted by plate count method.

*Cell viability and LIVE/DAED assay*

The cell viability following treatment with NSAgNC was measured by MTT and LIVE/DAED kit assay. Cells (3 mL, $10^7$ CFU/mL) treated with NSAgNC (0–2.0 mg/mL) were separated and incubated with MTT solution at 37±1 °C for 4 h. After incubation, cells were collected by centrifugation (10,000 rpm, 10 min) and dissolved in formazan solubilization buffer. The absorbance of the supernatant was measured at 590 nm using a UV-vis spectrophotometer (Jasco, V650 model). The killing efficiency was determined as

Killing efficiency (%) = $[(OD_{590\ \text{negative control}} - OD_{590\ \text{treated}})/ (OD_{590\ \text{negative control}} - OD_{590\ \text{positive control}})] \times 100$, where negative and positive controls correspond to cells without any treatment and 70% isopropyl alcohol treated cells, respectively.

LIVE/DEAD assay of the treated cells were measured by staining with SYTO 9 (excitation/emission at 480/500 nm) and Propedium iodide (PI; excitation/emission at 535/617 nm). Both control and treated cells were stained with LIVE/DEAD kit (Invitrogen, CA) following the manufacturer's instructions and images were recorded on a fluorescence microscope (Olympus BX-61). The cell viability was then measured by counting the green and red cells in the microscopic fields. SYTO 9 is permeable in both live and dead bacteria and stain green fluorescent color. However, propidium iodide is only penetrated into the compromised cells owing to their altered membrane potential and exhibit red fluorescence. This simultaneously diminishes the fluorescence properties of SYTO 9. Live bacteria therefore strain green, while dead bacteria exhibit strong red emission.

*Outer membrane destabilization assay*

To elucidate the membrane damage and release of intracellular contents, NSAgNC treated cells were collected and resuspended in same volume of K-media (2.4 g KCl, and 3.1 g NaCl per litre) containing 0.1% sodium dodecyl-sulphate (SDS) followed by incubation for 2 h. The concentration of proteins in the supernatant was then measured spectrophotometerically.

*Alteration of cellular morphology*

The alteration of cellular morphology after treatment with NSAgNC was observed using transmission electron microscopy (TEM, JEOL JEM 2010) images. Bacterial cells were thoroughly washed with phosphate buffer (50 mM, pH 7.2), and then fixed with 2.5% glutaraldehyde solution for 5 h. The cells were then washed thrice with the same buffer followed by dehydration with graded ethanol series (40-100%). The dehydrated cells were drop casted on carbon-coated copper grid, and micrographs were recorded on a HRTEM instrument.

*Intracellular reactive oxygen species (ROS) and glutathione (GSH)* m*easurement*

Cells following treatment with NSAgNC were incubated with $H_2$-DCFDA in sterile phosphate buffer (50 mM, pH 7.0) and the fluorescence intensities of the cell suspensions were recorded using a Varian Eclips spectrofluorometer with excitation and emission at 488 and 525 nm, respectively.

The NSAgNC mediated oxidation of glutathione (GSH) was determined by 5,5′-dithio-bis-(2-nitrobenzoic acid) (DTNB) assay, which reacts with thiol to produce yellow product. Cells following treatment with NSAgNC were collected and lysed. The cell lysate (360 µL) was then mixed with 628 µL of Tris-HCl (pH 8.3) and 12 µL of 100 mM DTNB solution and incubated for 30 min in dark at 30 ± 2 °C. The absorbance of the reaction mixture was measured at 412 nm using U-vis spectrophotometer. Untreated and $H_2O_2$ (1 mM and 10 mM) treated cells were served as negative and positive control, respectively.

*Genomic DNA isolation*

The genomic DNA was isolated using the standard phenol-chloroform method [1]. In brief, 2 mL of the freshly grown bacterial culture was treated with NSAgNC (0–2.0 mg/mL) for 5 h. Cells were then collected by centrifugation (10,000 rpm, 15 min), washed with phosphate buffer (50 mM, pH 7.2) and resuspended in 890 µL of lysis buffer (50 mM Tris pH 8.0, 10 mM EDTA, 20% sucrose, 0.5% Triton X-100 and 100 µg/mL lysozyme) by gentle mixing. 100 µL of 10% SDS and 10 µL of Proteinase K (10 mg/mL) were added to the cells and incubated at 37 ºC for 1 h. 1 mL of phenol-chloroform (1:1) mixture was then added into the contents and incubated at 30 ºC for 5 min. Following incubation, it was then centrifuged at 10,000 rpm for 10 min at 4 ºC. The highly viscous jelly like supernatant was collected in a fresh tube and the process was repeated once with phenol-chloroform mixture. The sample was subsequently centrifuged at 10,000 rpm for10 min and supernatant was collected. 100 µL of 5 M sodium acetate solution was added into the supernatant and mixed gently by inverting the tube 2–4 times. After addition of 2 mL of isopropanol a white precipitation of DNA was obtained, which was collected by centrifugation at 5,000 rpm for 10 min. The pellet was subsequently collected and washed with 70%

ethanol. The pellet was then air dried for 5 min and suspended in 200 µL of TE buffer (50 mM Tris, pH 8.0 and 10 mM EDTA). The concentration of DNA was measured using a spectrophotometer at 260/280 nm and further analysed by 1.5% agarose gel electrophoresis followed by staining with ethidium bromide. The untreated culture was served as control and the DNA pattern of both treated and untreated cell was finally compared to measure the DNA damage due to NSAgNC treatment.

*Plasmid DNA isolation*

The plasmid DNA was extracted following the protocol of Holmes and Quigley [2]. 2 mL of freshly grown culture was treated with NSAgNC as described above and cell pellet was collected by centrifugation at 10,000 rpm for 15 min at 4°C. The pellet was washed with STE buffer (1M NaCl, 50 mM Tris-HCl pH 8.0 and 10 mM EDTA) and resuspended in 200 µL of TEG buffer (50 mM Tris-HCl pH 8.0, 10 mM EDTA, 0.5% Trinton X-100, and 200 mM glucose) containing 10 µL lysozyme (20 mg/mL) and 20 µL $ZnCl_2$ (1% in double distilled $H_2O$) and incubated for 5 min at 30 °C. Following incubation, 400 µL of freshly prepared 0.2 M of NaOH solution containing 1% SDS was added into the content and kept for 10 min on ice. Ice cold 300 µL of ammonium acetate solution (7.5 M, pH 7.8) was then added and incubated further for another 10 min. Upon completion of incubation, supernatant was collected by centrifugation (14,000 rpm for 15 min). 1 mL isopropanol was then added into the supernatant and incubated for 40 min at 30 °C followed by centrifugation at 14,000 rpm for 10 min. The pellet was collected, washed with 70% ethanol and air dried. Finally the pellet was dissolved in 50 µL of TE buffer (50 mM Tris-HCl, pH 8.0 and 10 mM EDTA). The concentration of plasmid DNA was estimated spectrophotometrically at 260/280 nm and DNA laddering pattern was analysed by standard 1.5% agarose gel electrophoresis followed by staining with ethidium bromide. The untreated culture was served as control and the plasmid DNA pattern of both treated and untreated cell was finally compared to measure the damage of plasmid due to NSAgNC treatment.

*Extraction of intra and extra cellular protein analysis*

Freshly grown bacterial culture (3 mL) was treated with different concentration of NSAgNC (0–2.0 mg/mL) as described above. The treated cells were centrifuged (10,000 rpm, 10 min) and supernatant containing extracellular proteins was collected. The concentration of extracellular proteins was then measured by Bradford assay [3] against standard protein solution.

To analyse the extracellular proteins, the cell pellet was dissolved in 1 mL of cell lysis buffer (50 mM Tris pH-8.0, 10% glycerol, 1% Triton X-100 and 1 mg/mL lysozyme) and incubate for 30 min at 30 °C under shaking (120 rpm). The cell suspension was then sonicated in an ice bath for 2 min (7 to 9 amp, Q500 Sonicator). Lysed cells were then separated by centrifugation at 10,000 rpm for 10 min and the

supernatant containing intracellular protein was collected. The protein concentration in the supernatant was measured by Bradford assay [3] and further analysed by standard 12% sodium dodecyl sulphate–polyacrylamide gel electrophoresis (SDS–PAGE).

## Results

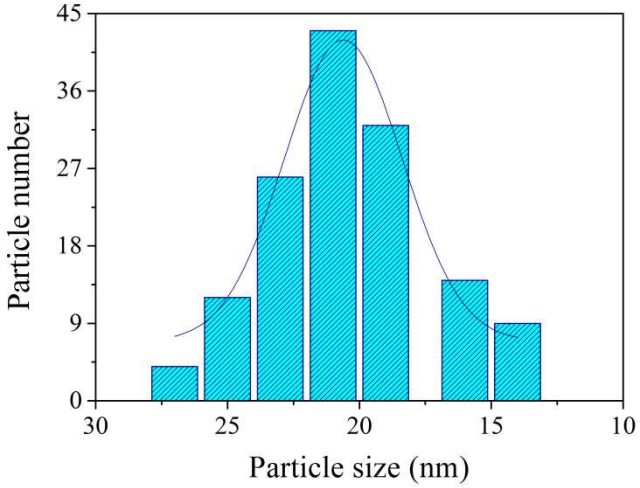


**Fig. S1:** Particle size distribution of silver nanoparticles synthesized on nano-silica.

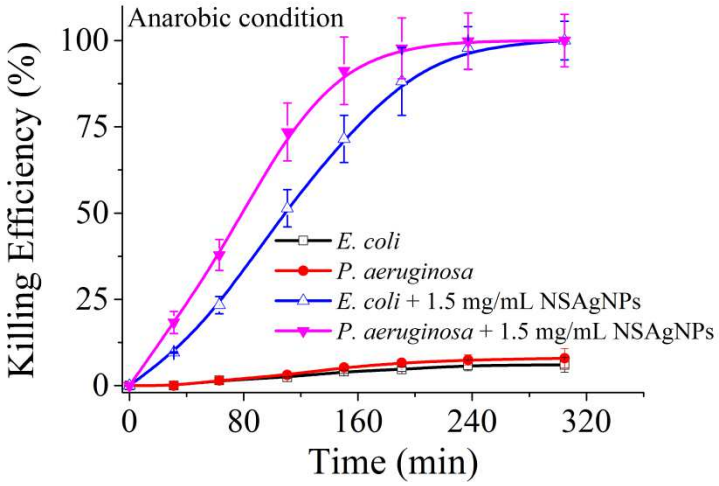


**Fig. S2:** Killing efficiency of NSAgNC under anaerobic condition. Data represent an average of five independent experiments ± SD shown by error bar.

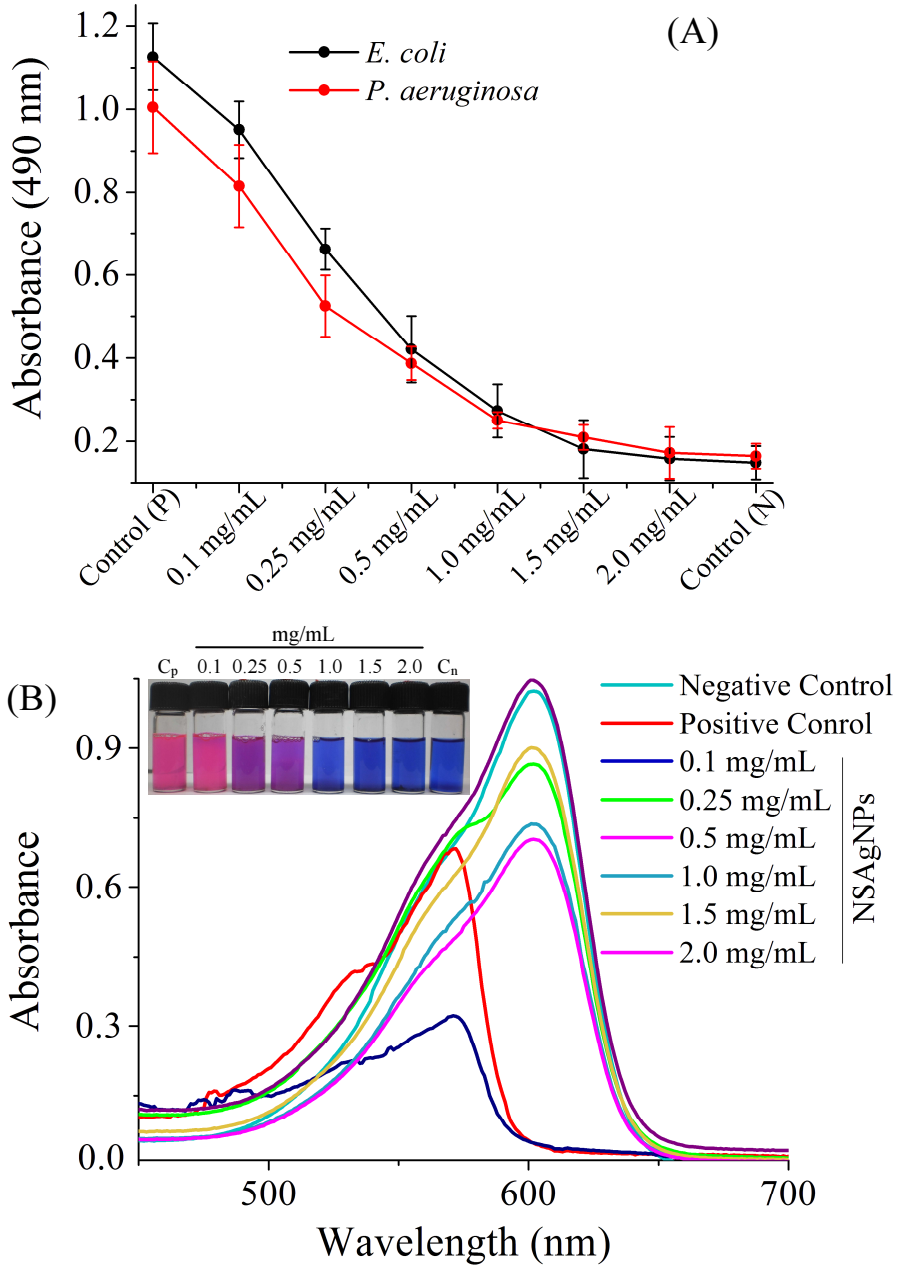


**Fig. S3:** Effect of NSAgNC on respiration chain dehydrogenase (A) in of *E. coli* and *P. aeruginosa* determined by conversion of INT to INF by viable cells; Metabolic activity (B) of *E. coli* measured by conversion resazurin to resorufin following treatment with different concentration of NSAgNC. Inset figure shows color images of metabolically active and inactive cells. Data represent an average of five independent experiments ± SD shown by error bar.

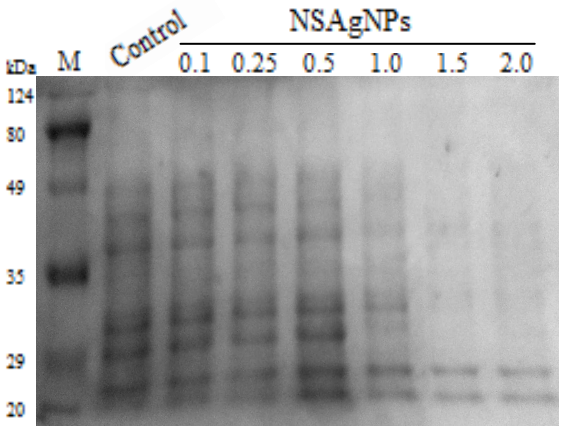


**Fig. S4:** SDS-PAGE protein profile analysis of *E. coli* following treatment with different concentration of NSAgNC for 5 h.

**Table S1**. Growth of *E. coli* or *P. aeruginosa* in NB with different concentrations of NSAgNC[a]

| Material | *E. coli* | | | | *P. aeruginosa* | | | |
|---|---|---|---|---|---|---|---|---|
| | 12 | 24 | 48 | 96 | 12 | 24 | 48 | 96 |
| Control | ++ | ++ | ++ | ++ | ++ | ++ | ++ | ++ |
| Nano-silica | ++ | ++ | ++ | ++ | ++ | ++ | ++ | ++ |
| 0.1 mg/mL NSAgNC | ++ | ++ | ++ | ++ | ++ | ++ | ++ | ++ |
| 0.25 mg/mL NSAgNC | + | ++ | ++ | ++ | - | + | ++ | ++ |
| 0.5 mg/mL NSAgNC | - | + | ++ | ++ | - | - | + | + |
| 1.0 mg/mL NSAgNC | - | + | + | ++ | - | - | - | - |
| 1.5 mg/mL NSAgNC | - | - | - | + | - | - | - | - |
| 2.0 mg/mL NSAgNC | - | - | - | - | - | - | - | - |

[a]NB liquid media was clear before inoculation with *E. coli* or *P. aeruginosa*; "–"no growth; "++" high growth; and "+" less growth.

**Table S2**: Extracellular protein concentration after treatment with different concentration NSAgNC for 8 h. The values are represented as mean ± SD of three individual experiments

| NSAgNC concentration (mg/mL) | Concentration of protein (mg/mL) | |
|---|---|---|
| | *E. coli* | *P. aeruginosa* |
| 0 | 0.02 ± 0.005 | 0.02 ± 0.002 |
| 0.1 | 0.04 ± 0.008 | 0.042 ± 0.003 |
| 0.25 | 0.08 ± 0.01 | 0.06 ± 0.005 |
| 0.5 | 0.17 ± 0.02 | 0.09 ± 0.01 |
| 1 | 0.35 ± 0.02 | 0.24 ± 0.015 |
| 1.5 | 0.41 ± 0.03 | 0.29 ± 0.02 |
| 2 | 0.43 ± 0.05 | 0.31 ± 0.02 |

**Table S3**: Effect of Surface charge on the antibacterial efficiency of NSAgNC against *E. coli*[*]

| pH values | 2.0 | 4.0 | 6.0 | 8.0 | 10.0 |
|---|---|---|---|---|---|
| Zeta potential of NSAgNC | 15.2 ± 2.5 | 8.5 ± 1.8 | 4.1 ± 1.2 | -3.5 ± 0.9 | -11.5 ± 2.5 |
| Killing efficiency (%) | 99.99 | 99.99 | 99.99 | 85.2 | 80.5 |

[*]The estimated zeta potential value of *E. coli* was -9.6 ± 0.7 mV

## References

[1] J. Sambrook, D.W. Russell, Molecular cloning; a laboratory manual, 3rd ed. Cold Spring Harbor Press: New York, 2001, Vol. 1.

[2] D. Holmes, M. Quigley, A rapid boiling method for the preparation of bacterial plasmids, Anal. Biochem. 114 (1981) 193-197.

[3] M.M. Bradford, Rapid and sensitive method for the quantitation of microgram quantities of protein utilizing the principle of protein-dye binding, Anal. Biochem. 72 (1976) 248–254.